JOURNAL OF MATERIALS SCIENCE 26 (1991) 5353–5366

Some structural, electrical and optical properties of copper phosphate glasses containing the rare-earth europium

J. M. ARZEIAN, C. A. HOGARTH
Department of Physics, Brunel University, Uxbridge, Middlesex, UB8 3PH, UK

Various properties of copper phosphate glass containing small amounts of the rare-earth europium have been investigated in the two glass systems Eu_2O_3–CuO–P_2O_5 and Eu_2O_3–CaO–CuO–P_2O_5. Density and molar volumes showed an increase as Eu_2O_3 replaced CuO and CaO in the glass compositions. Enhanced reduction from Cu^{2+} to Cu^{+} valency states of the ions in the glasses due to the presence of europium has been inferred from the results of electron spectroscopy for chemical analysis, and confirmed by results of electron spin resonance measurements. Corresponding electrical and optical band-gap characteristics, however, showed little systematic variation. The tetrahedral structure of P_2O_5 appeared to dominate the structural characteristics and infrared behaviour of the glass. The results are interpreted in terms of molecular structure, electronic configuration and small polaron hopping models. The role of europium in the glass is discussed.

1. Introduction

Oxide glasses containing transition metal ions have been studied for some time and the existence of relative proportions of the ions in different valency states has been used to explain electronic conduction, as the electrons transfer from ions in one valency state to ions in a higher valency state using as a model a hopping mechanism involving small polarons [1].

Transition metals contain a partially filled 3d shell in their electronic configuration. Rare-earths (lanthanides) contain a partially filled 4f shell. So glasses containing rare-earth ions may also exhibit different valency states and may contribute to electronic conduction.

Most research has been carried out on transition metal oxide glasses with added lanthanides from either end of the rare-earth series, e.g. cerium with two 4f electrons, or praseodymium with three 4f electrons, at one end of the series, and erbium with eleven 4f electrons, or lutetium with fourteen 4f electrons, at the other end of the series, in order to investigate how the addition of any of these might control the properties of the glass [2, 3]. It has been found that the presence of even a small quantity of a rare-earth oxide can dramatically alter such properties of the glass as its electrical conductivity, optical absorption and infrared behaviour.

Europium lies exactly half-way along the lanthanide series with its 4f shell exactly half-filled with seven 4f electrons. It was thought to be of interest to investigate the effect of adding europium to both the copper phosphate and copper calcium phosphate glass systems. It was predicted that perhaps the half-filled 4f shell being more stable, and considerably shielded by outer electron shells might result in behaviour more like that of a crystal with sharp optical absorption edge, but have little additional effect on such properties as the electrical conductivity, etc.

2. Experimental techniques

2.1. Preparation of glass

Glasses of composition $Eu_2O_{3(x)}$–$CuO_{(35-x)}$–$P_2O_{5(65)}$ (Series I) and $Eu_2O_{3(x)}$–$CaO_{(10-x)}$–$CuO_{(25)}$–$P_2O_{5(65)}$ (Series II) were prepared, where the compositions are given in mol % and $0 \leqslant x \leqslant 10$ mol %. It was thought that as the europium was increased in Series I glasses, the decrease in copper in the network might be masked. So a second series was prepared in which the europium was increased against a corresponding decrease in calcium, with copper concentration held constant (Series II), the oxides of the materials being used for the glass preparation in each case.

The oxide components were carefully weighed out and mixed in alumina crucibles and pre-heated in a furnace at 300 °C for 1 h, and then melted in another furnace at 1100 °C for 3 h where the melts were stirred from time to time. Finally the glass was poured on to a stainless steel plate and cast into disc-shaped samples, some unannealed and others annealed at 300, 400 and 500 °C, respectively, for 1 h. The samples were kept in a desiccator to prevent moisture absorption.

2.2. Density and molar volume measurements

The density of the glass samples was measured by a simple Archimedes process [4] suspending the glass discs by fine platinum wire and using ethylmethylketone (C_2H_5–CO–CH_3) of relative density 0.805 at 20 °C as the reference immersion liquid. The molar

0022–2461/91 $03.00 + .12

volumes were then calculated from the molecular weights and the densities, and the effects of annealing were also studied.

2.3. X-ray crystallography

The X-ray crystallographic investigation was carried out using the Debye–Scherrer technique in order to establish that a representative finely powdered sample of the glass was amorphous and not crystalline. At the same time a sample of crystalline Eu_2O_3 powder was also subjected to the same test for comparison.

2.4. Electron spectroscopy for chemical analysis (ESCA)

This is also known as X-ray photo-electron spectroscopy (XPS). ESCA is an analytical technique for studying X-ray photo-electron emission from samples irradiated typically by AlK_α X-rays in a vacuum and swept by a strong electric field. The resulting emitted electrons are energy-analysed, as they carry information about the energy states they have left behind. The ESCA spectrometer recorder provides a spectrum of the emission events as a continuous trace of kinetic energy, E, over the range 300–1550 eV. A series of peaks appear as various s p d energy levels are excited at various binding energies. Some of these are split on ionization giving $p_{1/2}$, $p_{3/2}$, $d_{3/2}$, $d_{5/2}$, $f_{5/2}$, $f_{7/2}$ levels known as doublets. A retarding field proportional to $1/E$ enables the events to be recorded. The vertical scale on the recorder chart is thus proportional to $N(E)/E$, where $N(E)$ is the density of states, so the chart represents an energy diagram of the sample. Using the ESCA X-ray apparatus (Perkin–Elmer KRATOS ES 300), ESCA scans were obtained for finely ground samples of the various crystal powders from which the glasses were made, and also for powdered samples of the glasses of various compositions. The scans were subsequently analysed and compared.

2.5. Electron spin resonance (ESR)

This is also known as electron paramagnetic resonance (EPR). Electron spin resonance is a branch of spectroscopy which deals with the study of systems containing unpaired electrons. As such it can be used to determine the relative proportions of transition metal ions in different oxidation states, as the paramagnetic ions respond to ESR and the diamagnetic ions such as Cu^+ do not. Landsberger and Bray [5] were the first to use ESR in a study of the concentration ratio C = [reduced valency ion]/[normal valency ion] in P_2O_5–V_2O_5 glasses. Moridi and Hogarth [6] were the first to study the reduced valency ratio $C = [Cu^+]/[Cu_{total}]$ in copper phosphate glasses using ESR techniques.

In the ESR method, samples are placed in the magnetic field, H, and subjected to a microwave radiation and a magnetic field sweep. Subsequent charted recordings indicate the resonance as the radiation energy disturbs the equilibrium and a map of the electron spin distribution may be obtained. This is in the form of the first derivative of paramagnetic susceptibility, $d\chi/dH$. From this the absorption curve may be derived using an integration procedure. ESR curves give a direct indication of the concentration of paramagnetic ions in the sample under investigation, resulting from unpaired electrons resonating in the applied fields.

Using the ESR Varian E3 spectrometer operating at 9.36 GHz frequency, ESR scans were obtained for finely ground samples of the glasses of various compositions, giving a direct indication of the concentration of Cu^{2+} (paramagnetic) ions in the glasses resulting from resonance of unpaired electrons. The glass samples were placed in turn in a quartz tube and individually weighed. Scans from each were compared with that from a copper sulphate crystal for which the spin concentration could easily be calculated. Spin concentrations in the glasses were then evaluated and the ESR results analysed.

2.6. Wet chemistry analysis

From ESR investigations the number of Cu^{2+} ions present in the glass samples can be determined. Also the total copper in the glasses may be calculated from molecular weight, or more accurately, by a wet chemical analytical method. Hence if $[Cu_{total}]$ and $[Cu^{2+}]$ are both known, the concentration of Cu^+ ions, $[Cu^+]$ may be calculated

$$[Cu_{total}] = [Cu^{2+}] + [Cu^+] \quad (1)$$

Also of interest is the reduced valency ratio C, where

$$C = \frac{[Cu^+]}{[Cu_{total}]} \quad (2)$$

The wet chemistry method used is a variation of the standard procedure described by Vogel [7] for determining the amount of copper in crystallized copper sulphate. A weighed quantity of glass powder is dissolved and potassium iodide added to obtain free iodine. The solution is titrated against N/10 sodium thiosulphate, with starch solution used for end-point determination and the concentration $[Cu^{2+}]$ in the glass sample determined. This method was used for glasses of all compositions, and values of $[Cu^+]$ and C were evaluated.

2.7. D.c. and a.c. conductivity

Electrical conductivity in copper phosphate glasses is believed to arise through hopping of electrons between ions in different valency states, i.e. the glass can carry a current due to an electron moving from a Cu^+ to a Cu^{2+} site. The conduction process can be regarded as hopping by small polarons because the polar nature of the glass matrix encourages the formation of such centres.

In the glasses containing europium, tests were carried out to establish this method of conduction in glasses of differing compositions.

The disc-shaped samples were ground and polished with diamond paste so that gold electrodes could be applied to each face, using a guard-ring configuration

on one face to minimize surface leakage current. D.c. current and voltage measurements were made with the samples at a vacuum of 10^{-5} torr (1 torr = 1.333 $\times 10^2$ Pa) and conductivity and electrical activation energy determined, for a range of temperatures between 20 and 300 °C, measured by means of a thermocouple.

A.c. measurements were made in a similar way using a Hewlett–Packard impedance analyser type 4192 A LF which gave a digital read out of capacitance and conductance of the sample, for an a.c. input signal of 500 mV_{rms} applied across it. The frequency was varied between 0.2 kHz and 10 MHz and the a.c. conductivity was investigated for the glasses.

2.8. Optical absorption edge

For amorphous semiconductor materials, and glasses which include rare-earths, the k-conservation rule governing optical interband transitions is relaxed and both direct and indirect, allowed and forbidden transitions may occur, the most likely for rare-earths in glasses being indirect and forbidden transitions involving the 4f levels.

The sharp absorption edge is likely to be considerably less sharp than for crystals, tailing well into the band-gap region. Two regions of the absorption edge may be considered.

(i) For high values of $\hbar\omega$, the photon energy, where the absorption coefficient $\alpha \geqslant 1 \times 10^4$ cm^{-1}, the Davis and Mott [8] reformulation of the Tauc rule [9] may be used for extended states

$$\alpha(\omega) = \frac{B(\hbar\omega - E_{opt})^n}{\hbar\omega} \quad (3)$$

where B is a determinable parameter, and E_{opt} is the optical energy gap.

(ii) For the more linear part of the absorption edge towards the lower values of α, the Urbach rule [10] may be used for optical transitions between localized states

$$\alpha(\omega) = \alpha_0 \exp\left(\frac{\hbar\omega}{\Delta E}\right) \quad (4)$$

where ΔE, the Urbach energy, may be estimated, and α_0 is a constant.

In order to investigate the absorption edge, thin blown films of samples of all the glasses were prepared. A portion of the glass was melted in a crucible and an alumina tube was quickly dipped into the molten glass and removed and a glass bubble formed by blowing into the tube. Small pieces of thin glass film of a few micrometres thickness were obtained in this way and then investigated for their spectral behaviour at room temperature using a Perkin–Elmer Lambda 9 UV/VIS/NIR spectrophotometer in the wavelength region 200–500 nm. Absorption spectra were obtained and from these the values of α, the absorption coefficient, ΔE, the Urbach energy or extent of the band-tailing, and E_{opt}, the optical energy gap, were determined.

2.9. Infrared absorption

Indirect transitions involving phonons to conserve energy, result in vibrations of the lattice in the infrared part of the spectrum. Using an infrared spectrophotometer, vibrations resulting from infrared radiation may be identified and analysed, and may yield valuable information regarding structure and bonding of the molecules of the material under investigation.

Samples of powdered glass from all the glass compositions were prepared using the KBr pellet technique, and infrared absorption spectra were obtained using a Pye Unicam SP 2000 infra-red double-beam spectrophotometer. Scans were obtained for wave numbers in the range 400–4000 cm^{-1}. These were compared with the infrared absorption spectra obtained from a sample of crystalline P_2O_5 in order to ascertain how much the phosphate bonds and bands influenced the glass structure.

3. Results and discussion

3.1. Density and molar volume

For both glass series there is a linear increase of both density and molar volume with increased europium content in the glass. Results are shown in Tables I and II for the various glass compositions of each series. The density increases are due to the higher europium content, while the molar volume increases are due to the larger ionic radii to be accommodated in the glassy matrix as Eu_2O_3 is added, in particular the O^{2-} ions of ionic radius 0.14 nm.

Annealing the glasses appeared to compact the structure and was manifested as an increase in density

TABLE I Compositions, densities and molar volumes for unannealed Series I glasses, $Eu_2O_{3(x)}$–$CuO_{(35-x)}$–$P_2O_{5(65)}$. Nominal values

Eu_2O_3 (mol %)	CuO (mol %)	P_2O_5 (mol %)	Relative density	Molar volume (cm^3)
0	35	65	2.91	41.3_2
1	34	65	2.95	41.5_9
2	33	65	2.99	41.9_3
3	32	65	3.06	41.8_7
5	30	65	3.15	42.4_3
10	25	65	3.38	43.5_9

TABLE II Compositions, densities and molar volumes for unannealed Series II glasses, $Eu_2O_{3(x)}$–$CaO_{(10-x)}$–$CuO_{(25)}$–$P_2O_{5(65)}$. Nominal values

Eu_2O_3 (mol %)	CaO (mol %)	CuO (mol %)	P_2O_5 (mol %)	Relative density	Molar volume (cm^3)
0	10	25	65	2.80	42.1_3
0.5	9.5	25	65	2.83	42.2_0
1	9	25	65	2.86	42.2_2
2	8	25	65	2.91	42.5_3
3	7	25	65	2.89	42.8_3
5	5	25	65	2.99	44.2_9
10	0	25	65	3.38	43.5_9

and a decrease in molar volume, which confirms the results of other workers in similar fields.

3.2. X-ray diffraction

An X-ray crystallographic investigation using the Debye–Scherrer technique revealed that the representative sample of finely powdered glass was amorphous and not crystalline as it produced no diffraction arcs on X-ray film after CuK_α irradiation for 6 h. A sample of crystalline Eu_2O_3 subjected to X-rays at the same time for 2 h did produce diffraction arcs, thus identifying the Eu_2O_3 as europium sesquioxide of lattice constant $a = 1.0866 \pm 0.05$ nm, using [11].

3.3. ESCA

It is appreciated that the soft X-rays penetrate the powdered glass samples to a depth of only a few micrometres. Nevertheless, some trends and compositional and structural indications may be observed, from the results.

General ESCA scans for samples of the crystal powders used in the glass manufacture enabled the relevant s d p, etc., peaks to be identified and then a detailed scan over a smaller range was taken. A general ESCA scan for crystalline CuO is shown in Fig. 1 and a detail of the Cu 2p doublet with its characteristic satellite peaks can be seen in Fig. 2. Similarly a general ESCA scan for crystalline Eu_2O_3 can be seen in Fig. 3 and a detail of the characteristic Eu 3d doublet is further identified in Fig. 4.

In the glass, more disorder is apparent in the detail scans. A typical general ESCA scan of a Series I glass is shown in Fig. 5, and detailed ESCA scans of the Cu 2p doublet for various glasses of Series I are shown in Fig. 6, and of the Eu 3d doublet for various glasses of Series I and II are shown in Fig. 7.

Comparison of ESCA detailed scans for the materials in the crystalline and the glassy chemical environments revealed a shift in binding energy. This is shown for Eu 3d in Fig. 8.

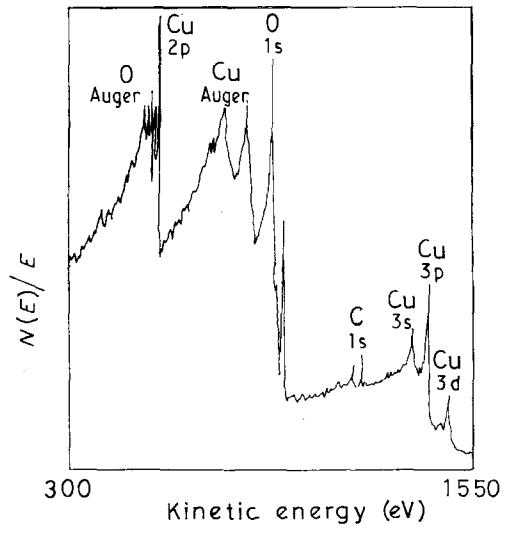

Figure 1 ESCA survey scan of crystalline CuO.

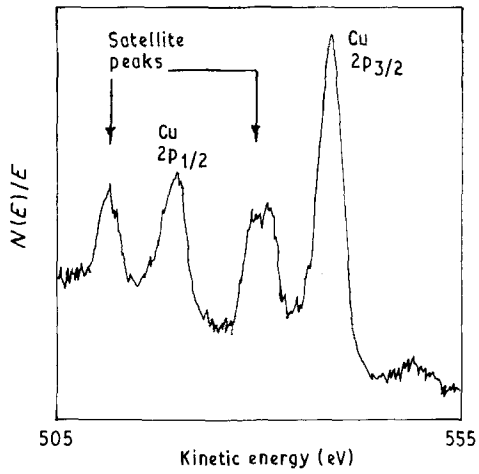

Figure 2 ESCA detail of Cu 2p doublet with satellite peaks in crystalline CuO.

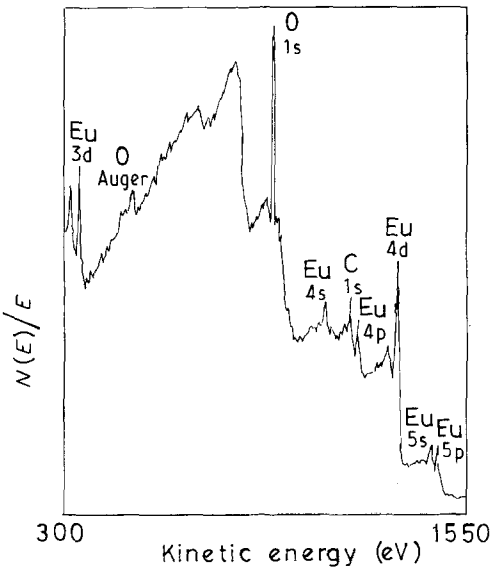

Figure 3 ESCA survey scan of crystalline Eu_2O_3.

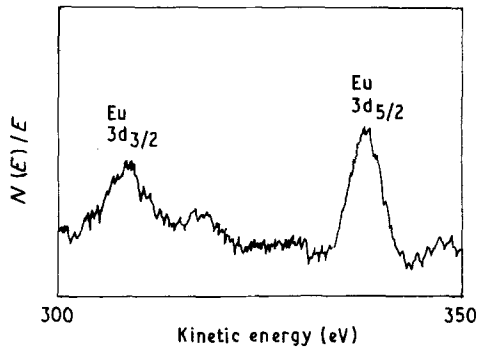

Figure 4 ESCA detail of Eu 3d doublet in crystalline Eu_2O_3.

ESCA findings are further discussed and summarized.

(i) Peak positions indicated s p d energy levels of components of the glass. In particular, the Eu 3d doublet, Cu 2p doublet, Ca 2p doublet and P 2p peaks were identified. Other peaks used as a reference were O 1s, C 1s, O Auger, etc.

(ii) Peak areas, i.e. the areas under the peaks on an expanded detailed scan over a small energy range,

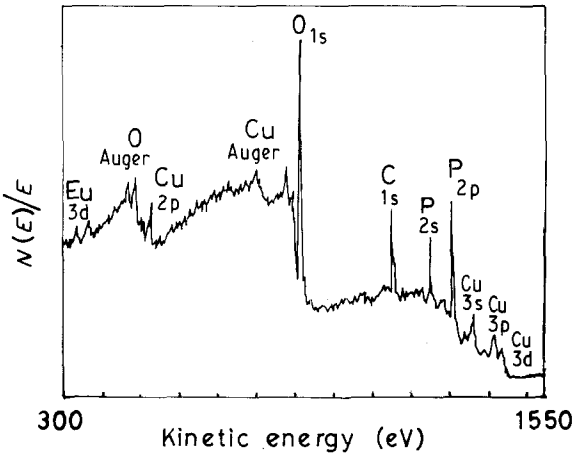

Figure 5 ESCA survey scan of a Series I glass, $Eu_2O_{3(3)}$–$CuO_{(32)}$–$P_2O_{5(65)}$.

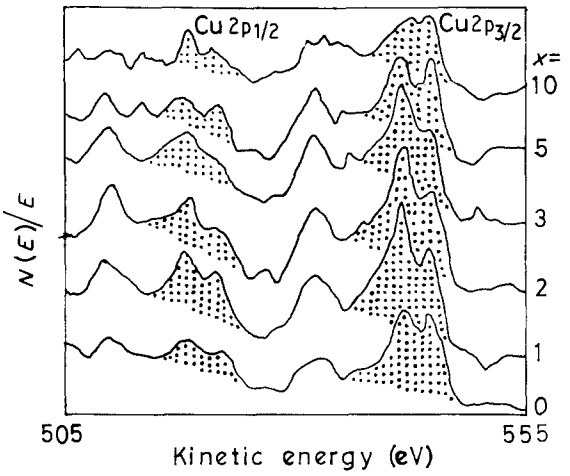

Figure 6 ESCA detail of Cu 2p doublet for various compositions in Series I glasses, $Eu_2O_{3(x)}$–$CuO_{(35-x)}$–$P_2O_{5(65)}$ (values of x shown in mol %).

showed distinctive characteristics and confirmed the glass composition by area comparison.

(iii) Peak shapes revealed some convolution in the Cu 2p peaks (Fig. 6) and could be interpreted as a possible reduction process $Cu^{2+} \rightarrow Cu^{+}$ as the glass composition is altered.

(iv) Peak broadening could also indicate more than one oxidation state (Fig. 7).

(v) Peak heights are proportional to the number of ionized atoms and can also be used for quantitative analysis and comparison, e.g. on a convoluted peak showing two oxidation states (Fig. 6).

(vi) A peak shift noted when comparing scans of crystalline and glassy states showed different binding energies for the two chemical environments. The Eu $3d_{5/2}$ peak and the Cu $2p_{3/2}$ peak both showed a decrease in binding energy from the crystalline to the glassy state, whereas Ca $2p_{3/2}$ showed an increase in binding energy, and the phosphorus peak stayed the same. This probably indicates a loss of some of the Eu and Cu bonds, and reflects the role of CaO as a network modifier in the glass.

Siegbahn [12] and co-workers first discovered that the binding energy of a core level varied with the

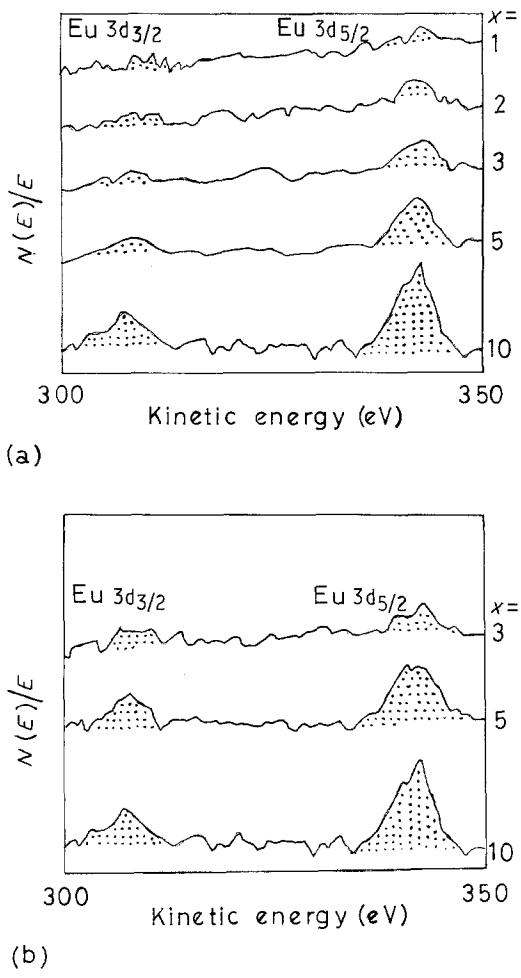

Figure 7 ESCA detail of Eu 3d doublet for various compositions (a) in Series I glasses, $Eu_2O_{3(x)}$–$CuO_{(35-x)}$–$P_2O_{5(65)}$; (b) in Series II glasses, $Eu_2O_{3(x)}$–$CaO_{(10-x)}$–$CuO_{(25)}$–$P_2O_{5(65)}$ (values of x shown in mol %).

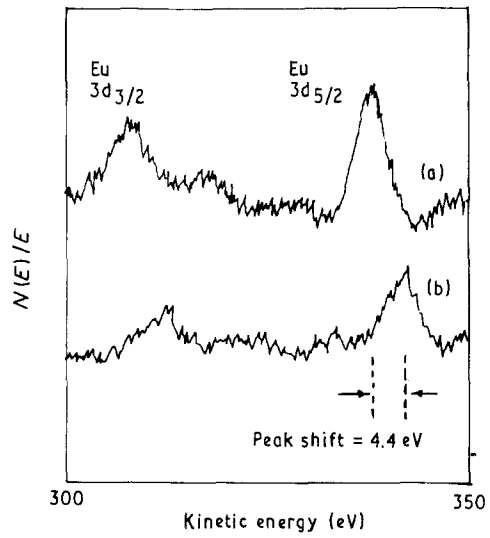

Figure 8 ESCA detail of 3d doublet in crystalline and glassy state showing peak shift (a) Eu 3d in crystalline Eu_2O_3, (b) Eu 3d in glass $Eu_2O_{3(10)}$–$CuO_{(25)}$–$P_2O_{5(65)}$.

chemical environment of an element, so that binding energy differences were chemical shifts. Briggs and Seah [13] discuss convolution in ESCA spectra and state that when atoms of an element are present as more than one type, i.e. in differing oxidation states or

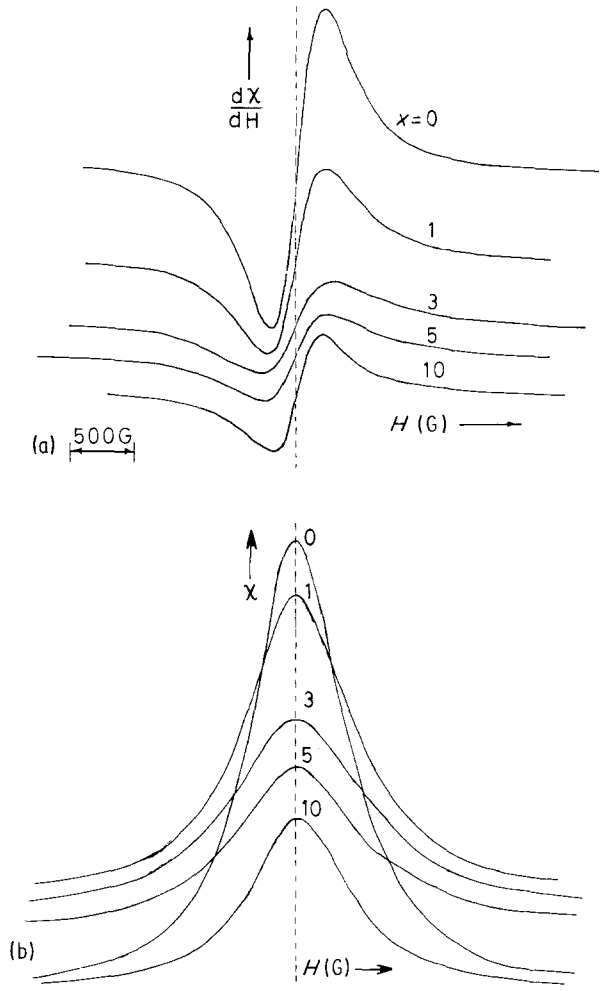

Figure 9 ESR spectra and corresponding absorption curves for some glasses of Series I, $Eu_2O_{3(x)}$–$CuO_{(35-x)}$–$P_2O_{5(65)}$ (values of x shown in mol %). (a) Derivative, (b) absorption.

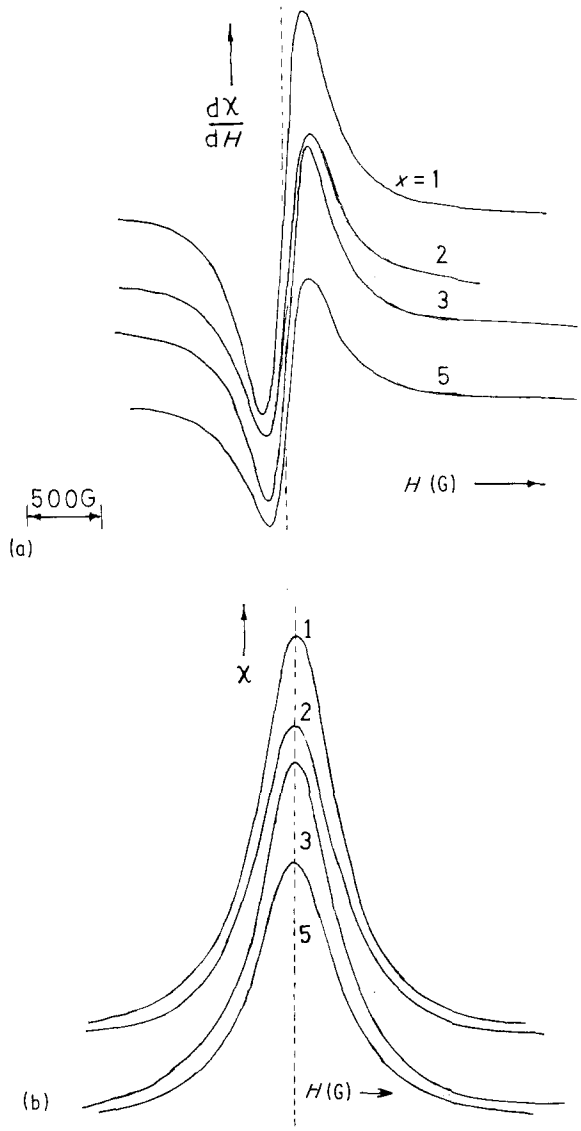

Figure 10 ESR spectra and corresponding absorption curves for some glasses of Series II, $Eu_2O_{3(x)}$–$CaO_{(10-x)}$–$CuO_{(25)}$–$P_2O_{5(65)}$ (values of x shown in mol %). (a) Derivative, (b) absorption.

chemical environments, they may have different binding energies and give rise to multiple ESCA peaks. Deconvolution is then necessary for accurate analysis using computer or Fourier transform methods. The technique of ESCA is thus seen as a useful and comparatively unexplored aid to the analysis of glass structure.

3.4. Electron spin resonance

ESR derivative and absorption spectra for glasses of Series I and II were obtained (Figs 9 and 10), and values for $[Cu_{total}]$, $[Cu^{2+}]$ and $[Cu^{+}]$ and also C, the reduced valency ratio, were determined. These results are tabulated in Tables III and IV and include the wet chemistry analysis of $[Cu_{total}]$. Results are also shown plotted in Figs 11–14. Spin density variation with Eu_2O_3 content is also shown in Fig. 15 for glasses of both series.

Some decrease in copper in the glasses is to be expected as the europium content is increased and replaces the copper, and the molecular weight of the glass alters accordingly, but there is a further splitting of the copper into its two valency states Cu^{2+} and Cu^{+} with the addition of europium to the glass. This is shown as a decrease in Cu^{2+} and a corresponding increase in Cu^{+} up to a certain level after which there is not much change. The addition of europium can be

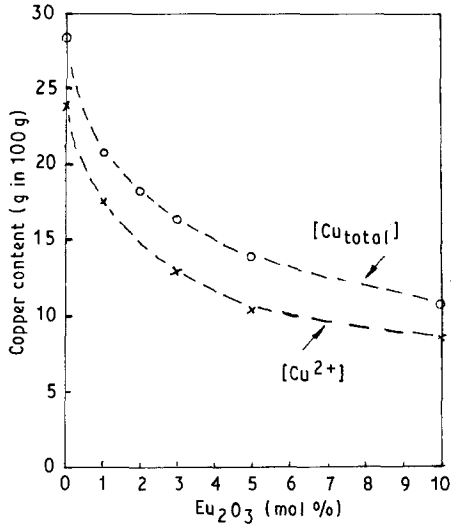

Figure 11 Decrease of Cu^{2+} ion concentration by ESR compared with total Cu concentration by wet chemistry for increasing Eu_2O_3 content in copper phosphate glasses containing europium (Series I).

TABLE III Reduced valency states results from titration and ESR for copper phosphate glasses containing europium, Series I, $Eu_2O_{3(x)}$–$CuO_{(35-x)}$–$P_2O_{5(65)}$

Eu_2O_3 (mol %)	CuO (mol %)	P_2O_5 (mol %)	Total Cu in 100 g glass (g), P[a]	Cu^{2+} in 100 g glass (g), Q[b]	Total Cu in 100 g glass before melting (g), R[c]	Cu^+ in 100 g glass (g), $P-Q$	$\frac{[Cu^+]}{[\text{Total Cu}]} = C$, reduced valency ratio, $\frac{P-Q}{P}$	Spin density of glass (10^{20} spins g^{-1})
0	35	65	28.0_0	23.7_0	18.5_2	4.3_0	0.15	22.3_8
1	34	65	20.5_0	17.4_6	17.5_9	3.0_4	0.15	16.4_9
2	33	65	18.3_5	–	16.7_0	–	–	–
3	32	65	16.4_6	12.9_8	15.8_5	3.4_8	0.21	12.2_6
5	30	65	13.5_2	10.1_8	14.2_5	3.3_4	0.24	9.6_1
10	25	65	10.3_1	8.4_9	10.7_8	1.8_2	0.18	8.0_2

[a] P from wet chemical analysis.
[b] Q from ESR measurements.
[c] R from original weighing.

TABLE IV Reduced valency states results from titration and ESR for copper phosphate glasses containing europium, Series II, $Eu_2O_{3(x)}$–$CaO_{(10-x)}$–$CuO_{(25)}$–$P_2O_{5(65)}$

Eu_2O_3 (mol %)	CaO (mol %)	CuO (mol %)	P_2O_5 (mol %)	Total Cu in 100 g glass (g), P[a]	Cu^{2+} in 100 g glass (g), Q[b]	Total Cu in 100 g glass before melting (g), R[c]	Cu^+ in 100 g glass (g), $P-Q$	$\frac{[Cu^+]}{[\text{Total Cu}]} = C$, reduced valency ratio, $\frac{P-Q}{P}$	Spin density of glass (10^{20} spins g^{-1})
0	10	25	65	18.1_2	16.7_9	13.4_9	1.3_3	0.0	15.8_5
1	9	25	65	15.3_5	11.6_0	13.1_6	3.7_5	0.24	10.9_5
2	8	25	65	13.7_0	10.6_4	12.8_4	3.0_6	0.22	10.0_5
3	7	25	65	11.9_4	10.7_6	12.5_4	1.1_8	0.10	10.1_6
5	5	25	65	10.7_4	8.6_0	11.9_8	2.1_4	0.20	8.1_2
10	0	25	65	10.3_1	8.4_9	10.7_8	1.8_2	0.18	8.0_2

[a] P from wet chemical analysis.
[b] Q from ESR measurements.
[c] R from original weighing.

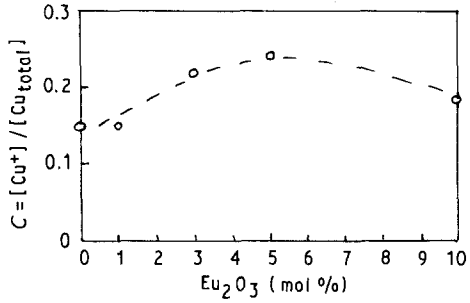

Figure 12 The relationship between Eu_2O_3 content and the reduced valency constant C for copper phosphate glasses containing europium (Series I).

said to enhance the formation of reduced valency states.

Various reasons have been put forward to explain this enhanced reduction of Cu^{2+} to Cu^+ which comes about by the addition of a rare-earth to a copper phosphate glass. There are three main suggestions for the origin of this effect.

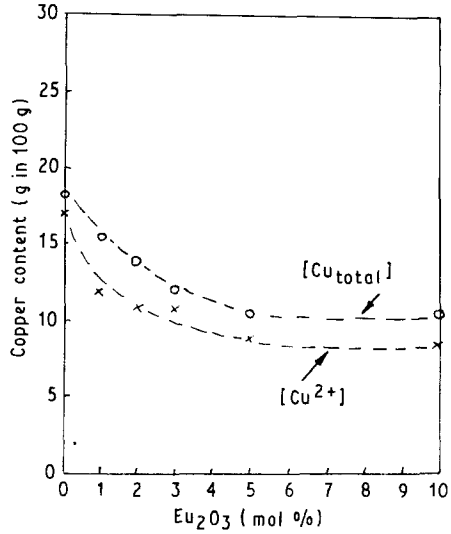

Figure 13 Decrease of Cu^{2+} ion concentration by ESR compared with total copper concentration by wet chemistry for increasing Eu_2O_3 content in copper calcium phosphate glasses containing europium (Series II).

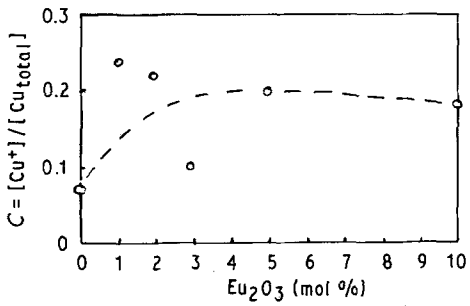

Figure 14 The relationship between Eu_2O_3 content and the reduced valency constant C for copper calcium phosphate glasses containing europium (Series II).

1. Processes involving redox phenomena between different elements in the glass.
2. Spin-spin interactions of various kinds.
3. Spin-lattice interactions, with the concept of cross-relaxation.

These are next discussed with particular regard to europium in the copper phosphate glass system.

3.4.1. Redox reaction

This type of reaction was suggested by Konstants and Vaivada [14] in 1981, e.g. if there are two elements in the system which form ions of variable valency, then interaction between them usually takes place as follows

$$Mn^{3+} + Ce^{3+} \rightleftharpoons Mn^{2+} + Ce^{4+} \quad (5)$$

This type of reaction was suggested by Mohammed-Osman *et al.* [15] for copper phosphate glasses containing Pr_6O_{11}

$$Cu^{2+} + Pr^{3+} \rightleftharpoons Cu^{+} + Pr^{4+} \quad (6)$$

However, for copper phosphate glasses containing Eu_2O_3, a reaction such as

$$Cu^{2+} + Eu^{3+} \rightleftharpoons Cu^{+} + Eu^{4+} \quad (7)$$

is not probable, because the europium ion is found in only two valency states, Eu^{2+} and Eu^{3+}, of which Eu^{2+} is the most stable and Eu^{3+} is paramagnetic and less stable, with an unpaired electron. The europium has not been found to exist as Eu^{4+}. Thus a redox reaction of the type suggested could only take place if Eu^{2+} was already present, i.e.

$$Cu^{2+} + Eu^{2+} \rightleftharpoons Cu^{+} + Eu^{3+} \quad (8)$$

and this would only be possible subsequent to a reaction such as

$$Eu^{3+} + e^{-} \rightarrow Eu^{2+} \quad (9)$$

because Eu_2O_3 is the prime constituent of the glass.

If there were a shift towards a diamagnetic or more stable state, as observed by Abdrakhmanov *et al.* [16] and Bogomolova [17] this might result in both $Cu^{2+} + e^{-} \rightarrow Cu^{+}$, and $Eu^{3+} + e^{-} \rightarrow Eu^{2+}$ occurring, the latter being more probable.

As the glass is manufactured, one would expect the copper to be present in the glass in its two valency states as this is the normal result for transition elements. Possibly the same thing occurs for the europium in the glass and if so, then there might in principle be some Eu^{2+} available to take part in a redox reaction

$$Cu^{2+} + Eu^{2+} \rightleftharpoons Cu^{+} + Eu^{3+} \quad (10)$$

On the other hand this reaction is considered unlikely, and is not in fact borne out by experiment, because the curves of reduced valency ratio show a flattening off rather than an increase, with increase of europium content in the glass.

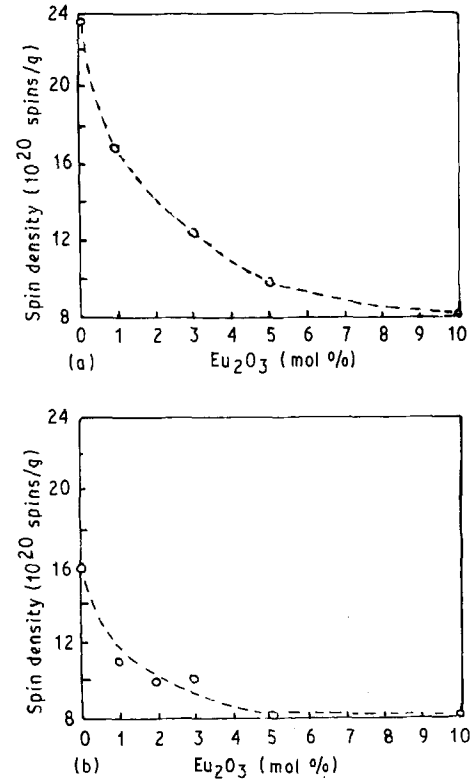

Figure 15 Spin density variation with Eu_2O_3 content (a) for copper phosphate glasses containing europium (Series I), (b) for copper calcium phosphate glasses containing europium (Series II).

3.4.2. Spin–spin interaction

Spin–spin interaction between paramagnetic particles depends on the orientation of their magnetic moments. Two types can be considered.

(i) Spin–spin exchange interactions between the paramagnetic ions which are producing the ESR line spectra, in this case the Cu^{2+} ions. This was suggested by Bogomolova *et al.* [18], i.e. that where the odd electron wave-functions on different orbitals overlap, then the unpaired electron spins are coupled by exchange forces. Exchange coupling allows the electrons on neighbouring lattice sites to exchange spin states rapidly as a result of the overlapping of the Cu^{2+} orbitals, (d electrons of the same spin). Working with vanadate glasses, Bogomolova [17] suggests that for V^{4+} ions, some redox reaction and some exchange clustering with Cu^{2+} ions takes place.

(ii) Spin–spin exchange interactions between paramagnetic ions which are not participating in the resonance absorption, in this case the Eu^{3+} ions. For the tri-valent rare-earth ions the orbital moments of the 4f

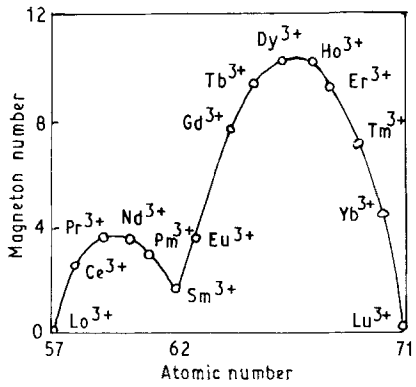

Figure 16 Magneton numbers of the lanthanide ions (M^{3+}) (reproduced from Bell and Lott [19]).

electrons contribute to their magnetic moments. Eu^{3+} is strongly paramagnetic, as can be seen from Fig. 16 above, reproduced from the book by Bell and Lott [19], and so could contribute to this type of spin–spin exchange interaction. However, the Eu^{3+} will not show up on a normal ESR spectrum. The electrons which contribute to the paramagnetic moment occupy the 4f orbitals and are shielded from electrostatic and bonding effects. The rare-earth ions exhibit strong spin-orbit coupling and are strongly coupled to the lattice vibrations. Spin–lattice relaxation problems are such that the spin-lattice relaxation time is very small at high temperatures and the ESR line spectra would be too broad to be detectable. It would be necessary to cool the lattice to liquid helium temperature for any ESR signal to be detectable. Nevertheless, although undetectable, the Eu^{3+} ion will exert a magnetic effect both on other Eu^{3+} ions and on the Cu^{2+} paramagnetic ions causing some orbital distortion.

3.4.3. Spin–lattice interactions and cross-relaxation

During the ESR event the magnetic field transfers the paramagnetic particles from the lower to the upper spin levels, and the transient excited state of the Cu^{2+} ion under the process of microwave radiation is observed. Vibrations of the lattice occur and these give rise to transitions, mainly in the opposite direction, i.e. they oppose this, and magnetic energy is lost as heat energy in the lattice. Line-width is partly dependent on lattice temperature. Cross-relaxation is a concept associated with various types of spin interactions and the corresponding time to relax back to a state of equilibrium, i.e. the relaxation time. Spin–spin interactions already discussed may both have the same relaxation time, whereas spin–lattice interactions, taking into account the lattice vibrations, will most likely have different relaxation times. Moreover some ions may have longer spin–lattice relaxation time than others. The net result of these effects will be an ESR spectrum of line-width proportional to say $\tau_1^{-1} + \tau_2^{-1}$ where τ_1 and τ_2 are relaxation times for spin–spin interaction, and spin–lattice interaction respectively, either of which may be dominant [20].

Thus of these three processes, the most likely to have contributed to ESR line broadening and reduction of signal in the case of europium are the latter two.

3.5. D.c. and a.c. conductivity

D.c. current–voltage tests enabled the conductivity of the glasses to be determined and hence the electrical activation energy, W. The conductivity varied from around 1×10^{-13} to $1 \times 10^{-9}\ \Omega^{-1}\ cm^{-1}$ over the temperature range of room temperature (20 °C) to about 300 °C. Graphs for all the glasses were very similar showing no systematic variation in conductivity with increased Eu_2O_3 content. Any small change there might have been was swallowed up by the sensitivity of the glass conductivity to temperature change. The electrical activation energy, W, varied from 0.9–1.3 eV with only little difference between glasses of each series.

A.c. conductivity tests showed conductivity to rise fairly linearly with temperature at low frequencies, but at higher frequencies above 1 MHz the conductivity became almost independent of temperature, as confirmed by the results of other workers [21]. The d.c. and a.c. conductivity results are shown together in Fig. 17 for a typical glass of each series, and it is clear that the d.c. conductivity can be regarded as a limiting case. The disorder temperature at which the change of slope manifests itself was around 427 K which is in reasonable agreement with other workers [22, 23], and led to 854 K as the value of the Debye temperature. The theoretical treatment of electrical conduction by means of a hopping process between ions in different valency states was substantiated as part of the conduction process in glasses. The a.c. conductivity variation with frequency at different temperatures is shown for a typical glass of each of Series I and

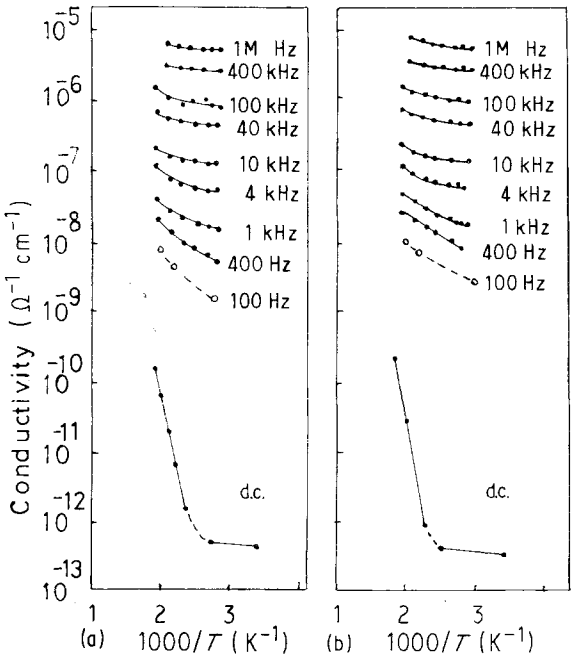

Figure 17 Variation of electrical conductivity with inverse temperature, a.c. and d.c. (a) for a Series I glass, $Eu_2O_{3(3)}$–$CuO_{(32)}$–$P_2O_{5(65)}$, (b) for a Series II glass, $Eu_2O_{3(3)}$–$CaO_{(7)}$–$CuO_{(25)}$–$P_2O_{5(65)}$.

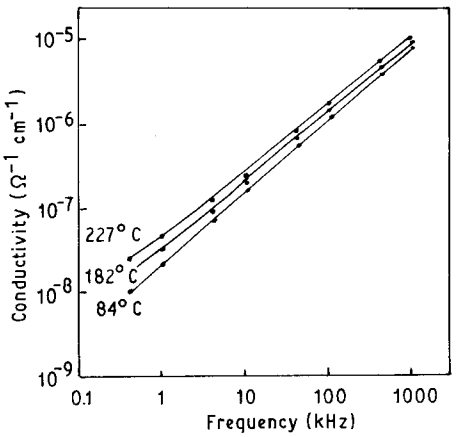

Figure 18 Variation of a.c. conductivity with frequency at different temperatures for a Series I glass, $Eu_2O_{3(5)}$–$CuO_{(30)}$–$P_2O_{5(65)}$.

Series II in Figs 18 and 19. From the slope the parameter, s, may be determined where

$$\sigma = A\omega^s \tag{11}$$

σ is the conductivity, A is a constant and s is an index. s was found to lie within the range $0.5 < s < 1$, with s about 0.68 at room temperature and slightly temperature dependent.

A problem found experimentally was the extreme sensitivity of the a.c. test results to reactive elements in the circuit such as the lead inductance, which was most difficult to eliminate when the samples were maintained in a vacuum during measurements and leads of significant length were necessary. For this reason the measurements, certainly above 100 kHz, shown in Fig. 17 should be regarded with caution. Extra spurious inductance was found to produce a vertical shift giving higher conductivity values for the same frequency, and masking the steep rise at higher temperatures. In some cases such errors could be substantial. Such problems have been discussed earlier by Jonscher [24].

The a.c. conductivity values for the various glass compositions showed little change with Eu_2O_3 increase in composition, any change being overshadowed by the extreme sensitivity of the glass to changes in frequency. It is thought that the shielding effect of the outer s and p electron shells on the 4f europium electrons could account for there being little change in conductivity with small changes in Eu_2O_3 content of the glass.

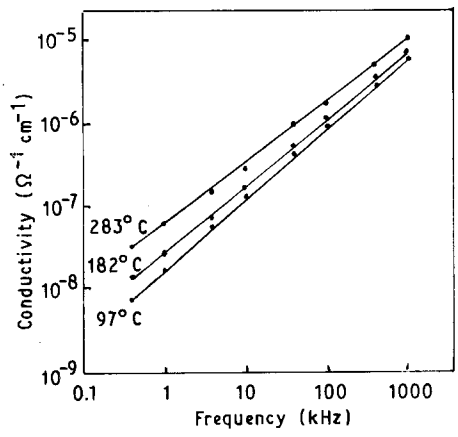

Figure 19 Variation of a.c. conductivity with frequency at different temperatures for a Series II glass, $Eu_2O_{3(5)}$–$CaO_{(5)}$–$CuO_{(25)}$–$P_2O_{5(65)}$.

3.6. Optical absorption

3.6.1. Absorption coefficient, α, and Urbach energy or band-tailing, ΔE

From the absorption spectra for samples of the glasses the absorption coefficient α was obtained (Fig. 20), and values of $\ln \alpha$ were plotted against photon energy $\hbar\omega$. The slope of these curves gives ΔE, the Urbach energy, or band-tailing using the Urbach relationship

$$\alpha(\omega) = \alpha_0 \exp\left(\frac{\hbar\omega}{\Delta E}\right) \tag{12}$$

where α_0 is a constant. ΔE was found to be around 0.5 eV for both glass series, there being little change in ΔE for small changes of Eu_2O_3 content.

3.6.2. Determination of the optical energy gap, E_{opt}

Assuming that absorption at higher α values was associated with indirect transitions, values of $(\alpha\hbar\omega)^{1/2}$ were plotted against the photon energy $\hbar\omega$ for $\alpha \geqslant 1 \times 10^4$ cm^{-1}. By extrapolation of the linear portions of these curves E_{opt} can be determined (Figs 21 and 22) for various glass compositions. E_{opt} was found to lie between 3.86 and 4.01 eV for Series I glasses and between 3.86 and 4.13 eV for Series II glasses. Values of E_{opt} did not appear to show any systematic variation with small changes of Eu_2O_3 content in the glass.

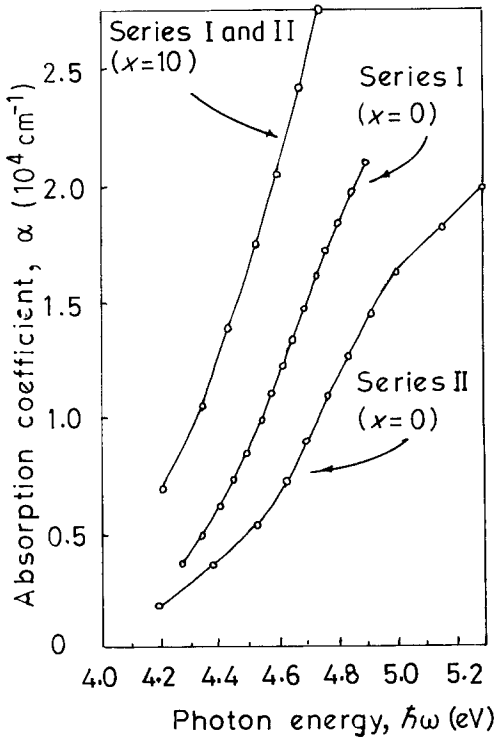

Figure 20 The absorption coefficient α as a function of photon energy $\hbar\omega$ for various glasses of Series I, $Eu_2O_{3(x)}$–$CuO_{(35-x)}$–$P_2O_{5(65)}$, and Series II, $Eu_2O_{3(x)}$–$CaO_{(10-x)}$–$CuO_{(25)}$–$P_2O_{5(65)}$ (values of x shown in mol %).

TABLE V Infrared absorption for Series I glasses, $Eu_2O_{3(x)}$–$CuO_{(35-x)}$–$P_2O_{5(65)}$

x (mol %)	Band positions (cm^{-1})							
0	495	700	775	900	1110	1260	–	3500
1	485	710	790	920	1100	1290	–	3500
2	500	725	785	925	1100	1285	–	3500
3	510	720	800	920	–	1300	–	3500
5	500	720	790	925	1100	1280	–	3480
10	485	720	800	925	1100	1280	–	3480

TABLE VI Infrared absorption for Series II glasses, $Eu_2O_{3(x)}$–$CaO_{(10-x)}$–$CuO_{(25)}$–$P_2O_{5(65)}$

x (mol %)	Band positions (cm^{-1})							
0	505	700	760	910	1100	1310	–	3500
1/2	485	710	770	920	1120	1315	–	3480
1	500	700	780	920	–	1310	–	3480
2	500	700	775	910	1120	1310	–	3500
3	485	705	760	910	–	1300	–	3490
5	505	705	775	910	–	1290	–	3490
10	485	720	800	925	1100	1280	–	3480

Determining E_{opt} in this way using the linear part of the curves seems to be satisfactory thus establishing $n = 2$ in the Mott and Davis extended states transition formulation

$$\alpha(\omega) = B\frac{(\hbar\omega - E_{opt})^n}{\hbar\omega} \quad (13)$$

The comparative insensitivity of these test results to small changes in Eu_2O_3 composition is thought to be due to the electron configuration of Eu, and the shielding effect of the s and p electrons on the 4f electrons, as suggested already for electrical conductivity results.

3.7. Infrared absorption

Spectra for both glass series were very similar, and not much variation in the bands was evident as the Eu_2O_3 content was increased in the glass, as shown in Fig. 23a and b and Tables V and VI. This suggests that the infrared spectra of the glasses are dominated by the spectral characteristic of P_2O_5 because this is a

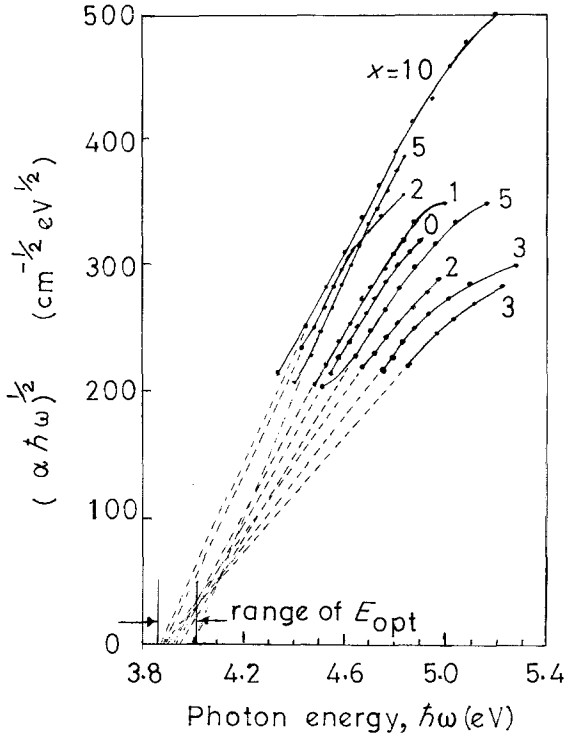

Figure 21 Determination of the optical energy gap by plotting $(\alpha\hbar\omega)^{1/2}$ as a function of photon energy $\hbar\omega$ for various glasses of Series I, $Eu_2O_{3(x)}$–$CuO_{(35-x)}$–$P_2O_{5(65)}$ (x in mol %).

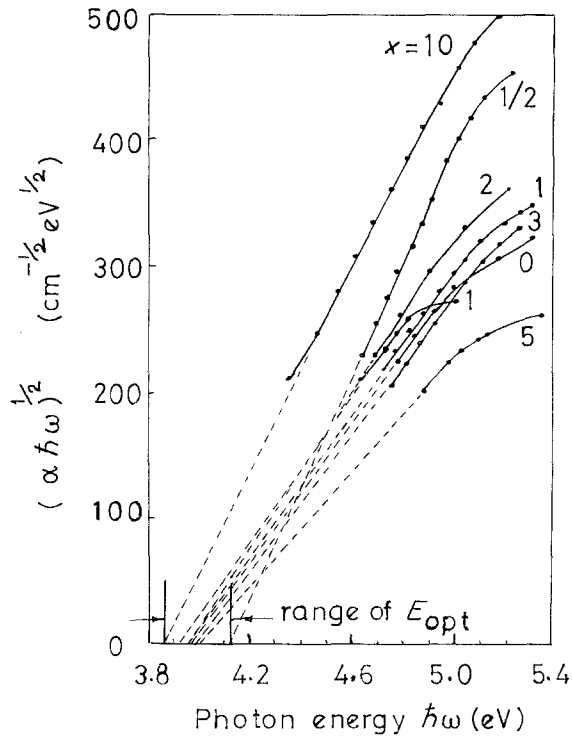

Figure 22 Determination of the optical energy gap by plotting $(\alpha\hbar\omega)^{1/2}$ as a function of photon energy $\hbar\omega$ for various glasses of Series II, $Eu_2O_{3(x)}$–$CaO_{(10-x)}$–$CuO_{(25)}$–$P_2O_{5(65)}$ (x in mol %).

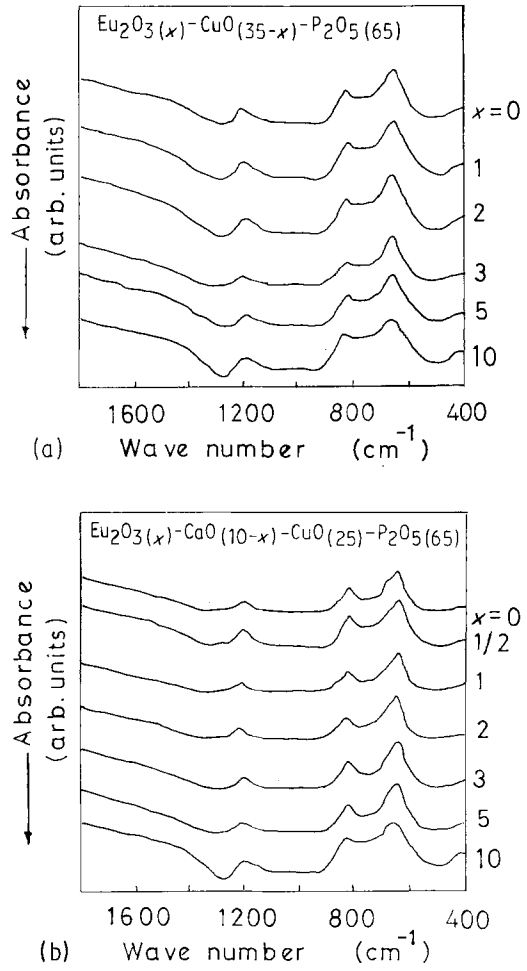

Figure 23 Infrared spectra (a) for glasses of Series I, (b) for glasses of Series II (x in mol %).

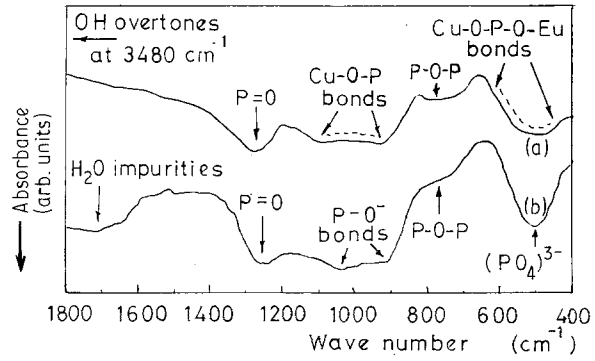

Figure 24 Comparison of infrared spectra for (a) glass $Eu_2O_{3(10)}$–$CuO_{(25)}$–$P_2O_{5(65)}$, and (b) crystalline P_2O_5. (The band positions are identified for P_2O_5, and the positions and nature of the bands for the glass are suggested.)

common constituent of both series. In spite of P_2O_5 being extremely hygroscopic an attempt was made to discern its spectral behaviour. This is shown in Table VII and a comparison with the infrared spectrum of one of the glasses is shown in Fig. 24.

The P_2O_5 bands can be approximately identified as follows using the results of previous workers in this field:

$(PO_4)^{3-}$ group	at 500 cm^{-1}
P–O–P ring frequency	at 780 cm^{-1}
$P–O^-$ stretching bond	from 900–1035 cm^{-1}
P=O double stretching bond	at 1260 cm^{-1}
H_2O water impurities, O–H	at around 1710 cm^{-1}
etc. with overtones	at 3480 cm^{-1}

There are two main differences when P_2O_5 infrared absorption is compared with the absorption spectra of the glass.

1. Firstly, the $(PO_4)^{3-}$ band at 500 cm^{-1} is replaced by a much broader band. This seems to be due to both the CuO in the glass and the europium, either separately, or together. CuO is known to have a fundamental band at 620 cm^{-1} so this may contribute to the broadening.

The rare-earths have absorption bands in the range 655–250 cm^{-1}. These rare-earth band positions were ascertained by Baun and McDevitt [25] who describe absorption bands for Eu_2O_3 at 630, 510, 475–250, 325 and 310 cm^{-1}. Thus the strong bands at 630 and 510 cm^{-1} may contribute to the observed broadening.

Some workers, e.g. Khan *et al.* [26], in a study of vanadate glasses, suggest a combined effect of all the constituents, with the formation in our case of Cu–O–P–O–Eu units, in the region of 450–600 cm^{-1} broadening and shifting the band. This suggestion could be consistent with the Reisfeld model of the Eu ion being at the centre of a distorted cube made up of four phosphate tetrahedra [27].

2. Secondly, the broadening and shift of the $P–O^-$ band and P=O band is noted in the glass spectra. Here perhaps the presence of the CuO in the glass has altered the stretching frequency. Other workers have noted a shift of band position when a transition metal oxide such as CuO is added to P_2O_5 glass, with broadening of the band. The suggestion is that a partial bond such as $P–O–Cu^+$ may be created in the region 900–1250 cm^{-1} and the band shifts with increasing CuO content.

In general it can be said that any small effect the rare earth oxide may have is swallowed up by the effect of the CuO in the glass composition, and the whole behaviour is dominated by the P_2O_5 which is the major constituent.

TABLE VII Infrared absorption for crystalline P_2O_5

	Band positions (cm^{-1})							
P_2O_5	505	–	780	900	1035	1260	1710	–

4. Conclusion

In this study various experiments have been carried out to determine the structural, electrical and optical properties of two series of copper phosphate glasses with small amounts of Eu_2O_3 introduced into the glass composition. The two series made up were $Eu_2O_{3(x)}$–$CuO_{(35-x)}$–$P_2O_{5(65)}$ and $Eu_2O_{3(x)}$–$CaO_{(10-x)}$–$CuO_{(25)}$–$P_2O_{5(65)}$ (x in mol %). In the first series Eu_2O_3 replaced the CuO and in the second series Eu_2O_3 replaced CaO in the glass. This second series with copper concentration held constant acted as a useful comparison during the investigation, although in general there was more disorder in this glass due to

incorporating a fourth constituent. However, CaO is a fairly inert network modifier.

In this final section an attempt is made to interpret and summarize the tests.

A representative sample of glass was tested by X-ray and confirmed as amorphous. In addition a sample of the crystalline Eu_2O_3 powder as used in the glass manufacture was precisely identified by the same X-ray method.

Density and molar volume tests gave results much as were expected, both density and molar volume increasing as Eu_2O_3 replaces CuO in the glass, Eu_2O_3 being of substantially greater molecular weight. There was a slight increase in density and decrease in molar volume with increased annealing temperature at a fixed glass composition, indicating that annealing the glass gives a more tightly packed and denser structure and reduces the interatomic spacings, generally producing a denser glass.

ESCA analysis of the glass gave interesting results. In spite of the fact that the ESCA X-rays only penetrate the finely powdered sample material to a depth of a few micrometres and so strictly affect only surface electron behaviour, nevertheless the results seem to be significant and can be used to give structural indications. Comparing the ESCA spectra of crystalline components used in the glass manufacture with the spectra of the glass itself proved a useful method for analysis. Peak area, peak shape, peak separation and peak heights were analysed. One result seemed to indicate a reduction of Cu^{2+} to Cu^{+} as Eu_2O_3 replaced CuO in the glass, by noting the apparent convolution of the Cu 2p doublet, and also a slight possibility of a similar reduction of Eu^{3+} to Eu^{2+}, by considering the Eu 3d doublet. Comparing the peak shift for spectra obtained in the crystalline and glassy states enabled the change in the binding energy to be calculated. Although these results can only be regarded as general trends, the indication seemed to be that, comparing the crystalline with the glassy state, Eu and Cu peaks showed a shift in binding energy in one direction while the Ca peak shifted in the opposite direction and the phosphorus peak stayed at about the same value. These results are consistent with small changes in bonding for Eu and Cu, the role of Ca as a network modifier, and the dominance of the phosphate tetrahedral bonding.

ESR analysis suggested that the reduced valency states of the ions Cu^{2+} and Cu^{+} were both present in the glass in varying amounts. Enhanced reduction from Cu^{2+} to Cu^{+} appears to maximize for small values of added Eu_2O_3 after which it falls off. This result confirms the predictions from the ESCA experiments resulting from the peak height analysis. C, the reduced valency ratio was determined from ESR analysis and the maximum for this is about 0.3 after which it appears to flatten off and drop slightly for further added Eu_2O_3.

Various suggestions as to how the presence of small quantities of Eu_2O_3 in the glass might enhance the reduction of Cu^{2+} to Cu^{+}, as revealed by ESR, were discussed. These were (i) redox reactions of the kind proposed earlier, considered possible but unlikely, (ii) spin–spin interactions between paramagnetic ions producing the ESR spectra, (the Cu^{2+} ions), or (iii) spin–spin exchange interactions between paramagnetic ions which do not participate in the ESR absorption (the Eu^{3+} ions). Also (iv) spin–lattice interactions generally produce line-broadening and loss of signal. It was suggested that all of these factors may contribute to the overall effect, though a redox reaction is considered unlikely unless there are Eu^{2+} ions already present in the glass. Both d.c. and a.c. electrical conductivity measurements were carried out on the glasses, the conduction theories invoked being those of Mott and Davis for a small polaron hopping mechanism. The d.c. case was seen as a limiting case for a.c. conduction according to the relationship $\sigma = A\omega^s$ and s was determined to be slightly less than 0.7. From d.c. tests the electrical activation energy, W, was determined and ranged from 0.8–1.3 eV for the various glass compositions. Conductivity was not especially sensitive to small changes in Eu_2O_3 composition in the glass, and this was attributed to the nature of the rare-earths in general in that their 4f electrons are shielded by outer electron shells, namely the $5s^2$, $5p^6$, and $6s^2$ electron shells. Also Eu has its 4f shell exactly half filled, which may contribute to extra stability.

The conduction mechanisms are considered to be electronic. It is well known that $CuO–P_2O_5$ glasses exhibit electronic or polaronic conduction. The addition of relatively small amounts of rare-earth oxides is unlikely to increase the contribution to the conductivity by ions because the Eu ion is large and unlikely to be mobile in the glassy matrix. Many structural studies of such glasses suggest that the Eu^{3+} ion would be fairly rigidly bound within the phosphate network.

Optical tests were carried out to determine band-gap characteristics, estimating the values of band gap and the extent of band-tailing from the measurements of the absorption edge. The Urbach energy, or band-tailing was around 0.5 eV and the optical energy gap was of the order of 3.95 eV.

These band-gap characteristics were found to be relatively insensitive to small changes in Eu_2O_3 composition. The reason for this is thought to be that the electrons responsible for the optical properties are the 4f electrons, and the 4f orbitals are very effectively shielded from outside influences by the overlying filled $5s^2$, $5p^6$, and $6s^2$ electron shells.

Infrared tests showed the dominance of the phosphate tetrahedra in lattice vibrations. Any small effect the rare-earth may have exerted was swallowed up by effects due to the copper in the glass, and both were dominated by the phosphate bonds.

Values obtained for W, the electrical activation energy, around 1.05 eV, and E_{opt}, the optical energy gap, around 3.95 eV, accord with the idea that in the limit, with the Fermi energy in the middle of the band-gap, the optical band gap would be twice the thermal activation energy, as for an intrinsic semiconductor. With the wide range of possible electron excitations in a glass, W is hard to define precisely on a band or density-of-states diagram, and is certainly likely to be less than $\frac{1}{2}E_{opt}$ as is the case in our glasses. The role

played by the rare-earth oxide Eu_2O_3 in $CuO–P_2O_5$ glass systems is thus seen to be an interesting one. While the presence of the europium appears to enhance reduction from Cu^{2+} to Cu^{+} valency states, and so is expected to assist in the conduction process, the basic electrical and optical properties of the glass remain relatively little affected by small additions of Eu_2O_3 to the glass.

References

1. N. F. MOTT, *J. Non-Cryst. Solids* **1** (1968) 1.
2. A. A. KUTUB, A. E. MOHAMMED-OSMAN and C. A. HOGARTH, *J. Mater. Sci.* **21** (1986) 3517.
3. C. ANANTHAMOHAN, C. A. HOGARTH and K. A. K. LOTT, *ibid.* **24** (1989) 4423.
4. G. W. MOREY, "Properties of Glass", 2nd Edn (Reinhold, New York, 1954).
5. F. R. LANDSBERGER and P. J. BRAY, *J. Chem. Phys.* **53** (1970) 2757.
6. G. M. MORIDI and C. A. HOGARTH, in "Proceedings of 7th International Conference on Amorphous and Liquid Semiconductors", edited by W. E. Spear (CICL, Edinburgh, 1977) p. 688.
7. A. I. VOGEL, "A text-book of quantitative inorganic analysis, theory and practice", 2nd Edn (Lowe and Brydone, London, 1951) p. 343.
8. E. A. DAVIS and N. F. MOTT, *Phil. Mag.* **22** (1970) 903.
9. J. TAUC, R. GRIGOROVICI and A. VANCU, *Phys. Status Solidi* **15** (1966) 627.
10. F. URBACH, *Phys. Rev.* **92** (1953) 1324.
11. J. D. H. DONNAY (ed.), "Crystal Data Determinative Tables", American Crystallographic Association Monograph No. 5 (American Crystallographic Association, Washington, DC, 1963).
12. K. SIEGBAHN, "ESCA applied to free molecules" (North Holland, Amsterdam, 1969).
13. D. BRIGGS and M. P. SEAH (eds), "Practical surface analysis by Auger and X-ray photoelectron spectroscopy" (Wiley, Chichester, 1983) Ch. 3.
14. Z. KONSTANTS and M. VAIVADA, *J. Non-Cryst. Solids* **45** (1981) 105.
15. A. E. MOHAMMED-OSMAN, K. A. K. LOTT, C. A. HOGARTH and M. A. HASSAN, *J. Mater. Sci.* **23** (1988) 1098.
16. A. S. ABDRAKHMANOV, Z. M. SYRITSKAYA and N. F. SHAPALOVA, *Izv. Akad. Nauk. SSSR* **7** (1971) 1240.
17. L. D. BOGOMOLOVA, *J. Non-Cryst. Solids* **30** (1979) 379.
18. L. D. BOGOMOLOVA, V. N. LAZUKIN and N. V. PETROVYKH, *Sov. Phys. Dokl. (USA)* **13** (1969) 679.
19. C. F. BELL and K. A. K. LOTT, "A modern approach to inorganic chemistry", 3rd Edn (Butterworths, 1972) p. 367.
20. S. A. AL'TSHULER and B. M. KOZYREV, "Electron paramagnetic resonance in compounds of transition elements", 2nd revised edn (Wiley, New York, 1974).
21. M. A. HASSAN, C. A. HOGARTH and G. R. MORIDI, *Phys. Status Solidi (a)* **101** (1987) 537.
22. G. R. MORIDI, PhD thesis, Brunel University (1975).
23. RAVISHANKAR HARANI and C. A. HOGARTH, *J. Mater. Sci. Lett.* **5** (1986) 492.
24. A. K. JONSCHER, *J. Non-Cryst. Solids* **8–10** (1972) 293.
25. W. L. BAUN and N. T. McDEVITT, *J. Amer. Ceram. Soc.* **46** (1963) 294.
26. M. N. KHAN, RAVISHANKAR HARANI, M. M. AHMED and C. A. HOGARTH, *J. Mater. Sci.* **20** (1985) 2207.
27. R. REISFELD, *Struct. Bond.* **13** (1973) 53.

Received 14 November 1990
and accepted 15 January 1991